Analytical Approach for Analysis of Nonuniform Lossy/Lossless Transmission Lines and Tapered Microstrips

Mohammad Hadi Eghlidi, Khashayar Mehrany, and Bizhan Rashidian

***Abstract*—In this paper, distribution of voltage along a general nonuniform transmission line is expanded in an appropriate form, and by employing an approach similar to conventional and modified differential transfer matrix methods already proposed for optical structures, analytical expressions are obtained for voltage/current distributions and reflection/transmission coefficients. This method shows great accuracy in different test cases and has been found to be superior to the well-known analytical method of small reflections. Notwithstanding, the overall accuracy of proposed approach is further improved by introducing the technique of multiple divisions. In particular, lossy/lossless tapered microstrip lines are examined, and excellent results are obtained. In deriving the formulation, a rigorous approach is followed and no simplifying assumptions are made; however, thanks to the analytical nature of the proposed method, high computational resources are not needed, and the results can be obtained extremely fast. This feature makes it suitable for optimization and synthesis of nonuniform transmission lines.**

***Index Terms*—Analytical methods, microstrip, nonuniform transmission line, tapered microstrip, transfer matrix, transmission line.**

I. Introduction

REGARDING the miniaturization and ever higher density packing of electronic devices, there is a high demand for having fast and reliable methods of analyzing the most widely used components of very large scale integration (VLSI) circuits and microwave integrated circuits. Nonuniform transmission lines are one of those components, and they have been extensively used by microwave engineers in many applications, including impedance matching [1], pulse shaping [2], antennas [3], pulsed circuits [4], filters [5], and analog signal processing [6]. Thanks to their ability to provide a smooth connection between high-density integrated circuits and their chip carriers, they also exist in many very large scale integration (VLSI) interconnections [7], [8]. As all of these applications call for an efficient, fast, and reliable method of analysis, many different techniques have been developed for analyzing nonuniform transmission lines over the past 60 years. The reflection coefficient of voltage/current along the transmission line can be expressed by a nonlinear Ricatti-type differential equation, whose general solution does not exist analytically [1]. This lack of general analytical solutions has spurred the use of different numerical techniques [9], [10] for analysis of the most general case. Notwithstanding, the theories of exponential [1], [11], [12], parabolic [13], [14], cosine squared [14], linearly tapered [15], and power-law transmission lines [16] are well established. However, finding an analytical solution for general nonuniform transmission lines is still commendable. Such a solution can be specifically useful in fast analysis, synthesis [17], [18], and optimization [19] of desired structures.

In this paper, a differential transfer matrix method (DTMM) is employed for analyzing tapered transmission lines, where, by expanding voltage distribution in terms of unknown coefficients, analytical formulas for voltage/current distributions and transmission/reflection coefficients are found. This proposed approach is capable of analyzing the most general nonuniform lossy/lossless transmission lines, whose characteristic impedance and propagation coefficient can both be position-dependent. Fortunately, high computational resources are not needed, and the proposed technique has a short run time. It should be noted that the DTMM has been previously reported for studying the wave propagation in one-dimensional (1-D) and nonhomogeneous isotropic [20]–[22] and anisotropic [23] optical structures. Furthermore, some special treatments in multisection structures are discussed, and new techniques of geometrically uniform and electrically uniform multiple divisions are introduced for improving the accuracy of the proposed method.

The organization of this paper is as follows. In Section II, the main formulation of the method for calculation of differential transfer matrix and voltage/current distributions is introduced. In Section III, reflection/transmission coefficients are derived, and some special cases are further discussed. In Section IV, the accuracy of the presented method and its superiority to the analytical small reflection method [1], [5] is proven by some numerical examples. In particular, tapered microstrip lines are investigated in Section V. Finally, conclusions are made in Section VI.

II. Analysis of Nonuniform Transmission Lines

The voltage wave in each point of a transmission line is composed of a right traveling wave and a left traveling wave. In a tapered transmission line, which is shown schematically in Fig. 1, the amplitudes of these waves are dependent on the coordinate,

Manuscript received April 17, 2006; revised July 16, 2006.

M. H. Eghlidi was with the Electrical Engineering Department, Sharif University of Technology, 11365-9363 Tehran, Iran. He is now with the Technical Faculty of Christian-Albrechts-Universität, D-24143 Kiel, Germany (e-mail: he@tf.uni-kiel.de).

K. Mehrany is with the Department of Electrical Engineering, Sharif University of Technology, 11365-9363 Tehran, Iran (e-mail: mehrany@sharif.edu).

B. Rashidian is with the Department of Electrical Engineering, the Institute for Nano Science and Technology, and the Center of Excellence for Nano Structures, Sharif University of Technology, 11365-9363 Tehran, Iran (e-mail: rashidia@sharif.edu).

Digital Object Identifier 10.1109/TMTT.2006.885565

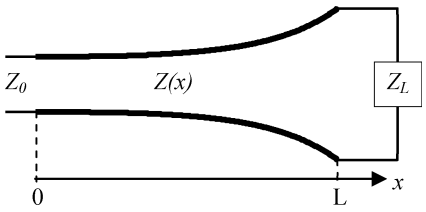

Fig. 1. Illustration of a tapered transmission line terminated with a matched load.

i.e., x. Here, the following form for the voltage distribution is expanded in terms of two forward and backward waves:

$$V(x) = A^+(x)\sqrt{Z(x)}\exp[-j\phi(x)] + A^-(x)\sqrt{Z(x)}\exp[+j\phi(x)] \tag{1a}$$

where $Z(x)$ is the characteristic impedance at point x, and $A^{\pm}(x)$ are unknown functions to be determined later. Also

$$\phi(x) = \int_0^x \beta(x')dx' \tag{1b}$$

in which β denotes the propagation constant.

It should be noted that the characteristic impedance and propagation constant could be complex to account for lossy structures. One can conclude the following form for the current distribution:

$$I(x) = A^+(x)\exp[-j\phi(x)]/\sqrt{Z(x)} - A^-(x)\exp[+j\phi(x)]/\sqrt{Z(x)}. \tag{2}$$

To find the unknown functions $A^{\pm}(x)$, we follow the differential method used in [20]–[24]. For this purpose, one can locally consider $A^{\pm}(x)$ and Z as piecewise constant functions that are equal to $A^{\pm}(x)$ and $Z(x)$ on the left side of the point x and $A^{\pm}(x+\Delta x)$ and $Z(x+\Delta x)$ on the right side of the same point. Then, the continuity of voltage at point x is written as

$$\begin{aligned} &A^+(x)\sqrt{Z(x)}\exp[-j\phi(x)] + A^-(x)\sqrt{Z(x)}\exp[+j\phi(x)] \\ &\quad = A^+(x+\Delta x)\sqrt{Z(x+\Delta x)}\exp[-j\phi(x)] \\ &\qquad + A^-(x+\Delta x)\sqrt{Z(x+\Delta x)}\exp[+j\phi(x)]. \end{aligned} \tag{3}$$

Further simplification of the preceding equation in the limiting case of $\Delta x \to 0$ yields

$$\frac{d\left[A^+(x)\sqrt{Z(x)}\right]}{dx}\exp[-j\phi(x)] + \frac{d\left[A^-(x)\sqrt{Z(x)}\right]}{dx}\exp[+j\phi(x)] = 0. \tag{4}$$

Similarly, using the continuity of current at point x and assuming $\Delta x \to 0$ lead to

$$\frac{d\left[A^+(x)/\sqrt{Z(x)}\right]}{dx}\exp[-j\phi(x)] - \frac{d\left[A^-(x)/\sqrt{Z(x)}\right]}{dx}\exp[+j\phi(x)] = 0. \tag{5}$$

Equations (4) and (5) can be written in the matrix form as

$$\frac{d}{dx}\mathbf{A}(x) = \mathbf{U}(x)\mathbf{A}(x) \tag{6}$$

in which $\mathbf{A}(x) = [A^+(x)\ A^-(x)]^{\mathrm{t}}$ and

$$\mathbf{U}(x) = -\frac{Z'(x)}{2Z(x)}\begin{bmatrix} 0 & \exp[+j2\phi(x)] \\ \exp[-j2\phi(x)] & 0 \end{bmatrix} \tag{7}$$

where $Z'(x)$ is the derivative of the function $Z(x)$.

The solution to (6) can be written as

$$\begin{bmatrix} A^+(x) \\ A^-(x) \end{bmatrix} = \mathbf{Q}_{0\to x}\begin{bmatrix} A^+(0) \\ A^-(0) \end{bmatrix} \tag{8}$$

where $\mathbf{Q}_{0\to x}$ is a 2×2 matrix and is referred to as the transfer matrix from 0 to x. This matrix can be approximately calculated by the following equation [20]–[24]:

$$\mathbf{Q}_{0\to x} = \exp\left[\int_0^x \mathbf{U}(x')dx'\right] = \exp[\mathbf{M}(x)] \tag{9}$$

in which $\exp(\mathbf{M})$ can be expanded as

$$\exp(\mathbf{M}) = \mathbf{I} + \sum_{n=1}^{\infty}\frac{1}{n!}\mathbf{M}^n. \tag{10}$$

However, noting that $\mathbf{U}(x)$ is an off-diagonal matrix, one can draw a conclusion in the form of (11), shown at the bottom of this page, where

$$m_{12}(x) = -\int_0^x \frac{Z'(x')}{2Z(x')}\exp[+j2\phi(x')]\,dx' \tag{12a}$$

$$m_{21}(x) = -\int_0^x \frac{Z'(x')}{2Z(x')}\exp[-j2\phi(x')]\,dx'. \tag{12b}$$

$$\mathbf{Q}_{0\to x} = \exp\left\{\begin{bmatrix} 0 & m_{12}(x) \\ m_{21}(x) & 0 \end{bmatrix}\right\} = \begin{bmatrix} \cosh\left(\sqrt{m_{12}(x)}\sqrt{m_{21}(x)}\right) & \frac{\sqrt{m_{12}(x)}\sinh\left(\sqrt{m_{12}(x)}\sqrt{m_{21}(x)}\right)}{\sqrt{m_{21}}} \\ \frac{\sqrt{m_{21}(x)}\sinh\left(\sqrt{m_{12}(x)}\sqrt{m_{21}(x)}\right)}{\sqrt{m_{12}(x)}} & \cosh\left(\sqrt{m_{12}(x)}\sqrt{m_{21}(x)}\right) \end{bmatrix} \tag{11}$$

Finally, it can be easily verified that

$$\begin{aligned} A^+(x) &= A_0^+ q_{11} + A_0^- q_{12} \\ &= A_0^+ \cosh\left(\sqrt{m_{12}(x)}\sqrt{m_{21}(x)}\right) \\ &\quad + A_0^- \frac{\sqrt{m_{12}(x)}\sinh\left(\sqrt{m_{12}(x)}\sqrt{m_{21}(x)}\right)}{\sqrt{m_{21}(x)}} \end{aligned} \tag{13a}$$

$$\begin{aligned} A^-(x) &= A_0^+ q_{21} + A_0^- q_{22} \\ &= A_0^+ \frac{\sqrt{m_{21}(x)}\sinh\left(\sqrt{m_{12}(x)}\sqrt{m_{21}(x)}\right)}{\sqrt{m_{12}(x)}} \\ &\quad + A_0^- \cosh\left(\sqrt{m_{12}(x)}\sqrt{m_{21}(x)}\right) \end{aligned} \tag{13b}$$

where $A_0^\pm = A^\pm(0)$ are constants, $m_{ij(}x)$'s are given by (12a) and (12b), and q_{ij}'s are the elements of the matrix $\mathbf{Q}_{0\to x}$. These equations together with (1) and (2) give a solution for voltage and current distributions.

III. Special Considerations

Here, reflection and transmission coefficients are derived, some modifications indispensable in analysis of cascaded structures are discussed, and, finally, the multiple division technique is introduced for augmenting the overall accuracy of the obtained results.

A. Reflection and Transmission Coefficients

The reflection and transmission coefficients of a tapered transmission line placed within the region of $0 < x < L$ are derived in this subsection. Assume that a right-traveling wave is incident upon the medium from the left boundary at $x = 0$. It can be shown that the reflection and transmission coefficients are respectively given by (14) and (15), shown at the bottom of this page, where q_{ij}'s are the elements of transfer matrix $\mathbf{Q}_{0\to L}$, m_{ij}'s are defined by (12a) and (12b), and $\Delta = |\mathbf{Q}_{0\to L}|$. Furthermore, r_L is the reflection caused by the mismatch at the end of tapered transmission line and is given by

$$r_L = \exp\left[-j2\phi(L)\right]\frac{Z_L/Z(L)-1}{Z_L/Z(L)+1} \tag{16}$$

in which Z_L is the load impedance connected to the end of the tapered line.

In the special case of using the tapered transmission line as a matching section in which there is no mismatch at the end of the tapered line or, equivalently, $Z_L = Z(L)$, r_L becomes zero, then (14) and (15) reduce to

$$R = -\sqrt{\frac{m_{21}(L)}{m_{12}(L)}}\tanh\left(\sqrt{m_{12}(L)}\sqrt{m_{21}(L)}\right) \tag{17}$$

$$T = \exp[-j\phi(L)]\sqrt{\frac{Z(L)}{Z(0)}}\frac{1}{\cosh\left(\sqrt{m_{12}(L)}\sqrt{m_{21}(L)}\right)}. \tag{18}$$

B. Cascaded Structures

In the case where N tapered transmission lines are connected to each other, the overall transfer matrix can be computed by using the following formula:

$$\mathbf{Q} = \mathbf{Q}_N \prod_{i=1}^{N-1} \mathbf{T}_i \mathbf{Q}_i. \tag{19}$$

Here, $\mathbf{Q}_i$ denotes the transfer matrix associated with the ith tapered section and can be calculated by using (11). Also, $\mathbf{T}_i$, which we refer to as the jump matrix, is associated with the interface between the two consecutive sections i and $i+1$. These jump matrices can be computed by pursuing the subsequent procedure.

Considering $x = x_i$ as the interface point between the two successive sections i and $i+1$ and writing down the continuity

$$\begin{aligned} R &= \frac{A^-(0)}{A^+(0)} \\ &= \frac{r_L q_{11} - q_{21}}{q_{22} - r_L q_{12}} \\ &= \frac{r_L \cosh\left(\sqrt{m_{12}(L)}\sqrt{m_{21}(L)}\right) - \sqrt{m_{21}(L)/m_{12}(L)}\sinh\left(\sqrt{m_{12}(L)}\sqrt{m_{21}(L)}\right)}{\cosh\left(\sqrt{m_{12}(L)}\sqrt{m_{21}(L)}\right) - r_L\sqrt{m_{12}(L)/m_{21}(L)}\sinh\left(\sqrt{m_{12}(L)}\sqrt{m_{21}(L)}\right)} \end{aligned} \tag{14}$$

$$\begin{aligned} T &= \exp\left[-j\phi(L)\right]\sqrt{\frac{Z(L)}{Z(0)}}\frac{A^+(L)}{A^+(0)} \\ &= \exp\left[-j\phi(L)\right]\sqrt{\frac{Z(L)}{Z(0)}}\frac{\Delta}{q_{22} - r_L q_{12}} \\ &= \exp\left[-j\phi(L)\right]\sqrt{\frac{Z(L)}{Z(0)}}\frac{1}{\cosh\left(\sqrt{m_{12}(L)}\sqrt{m_{21}(L)}\right) - r_L\sqrt{m_{12}(L)/m_{21}(L)}\sinh\left(\sqrt{m_{12}(L)}\sqrt{m_{21}(L)}\right)} \end{aligned} \tag{15}$$

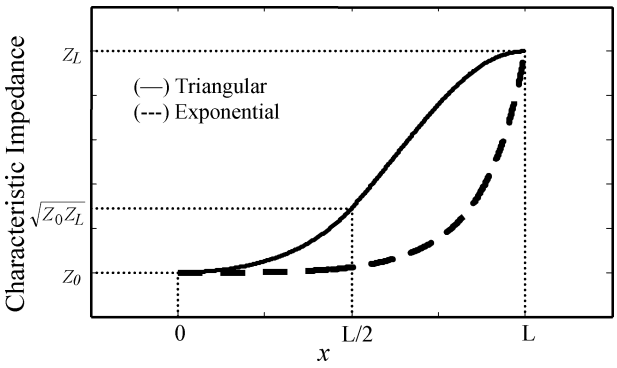

Fig. 2. Illustration of tapered lines with triangular and exponential distributions used in the examples.

condition of voltage and current distributions at the interface result in

$$\begin{bmatrix} A^+\left(x_i^+\right) \\ A^-\left(x_i^+\right) \end{bmatrix} = \mathbf{T}_i \begin{bmatrix} A^+\left(x_i^-\right) \\ A^-\left(x_i^-\right) \end{bmatrix} \tag{20}$$

where x_i^- and x_i^+, respectively, refer to the points just before and after the point x_i and $\mathbf{T}_i$ is the jump matrix of the ith interface given by (21), as shown at the bottom of this page, where one reference point, i.e., $x = 0$, has been chosen for all constituent sections.

On the other hand, each tapered section can have its own reference point, i.e., $x = x_{i-1}$, for the ith section. In this case, the continuity of voltage and current in an arbitrary interface point x_i leads to a different jump matrix given by (22), as shown at the bottom of this page.

C. Technique of Multiple Divisions

It will be shown in Section IV that, as the contrast of $Z(x)$ within the analyzed tapered line increases, the accuracy of the presented method declines. However, the whole tapered line can be divided into multiple divisions, each of them forming a subsection whose impedance profile $Z(x)$ is of lower contrast.

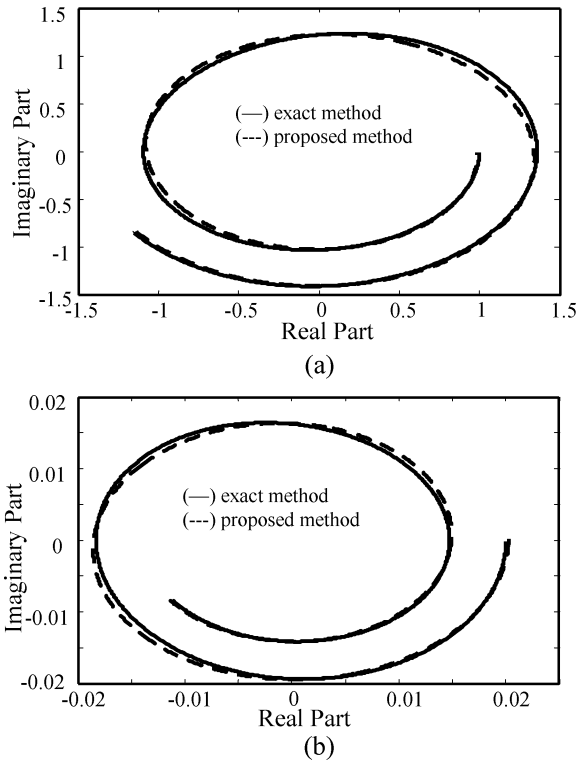

Fig. 3. Polar locus of voltage and current of triangular tapered line for $L/\lambda = 1.4$, $Z_0 = 50$, and $Z_L = 100$. (a) Voltage. (b) Current. Here, the voltage is normalized to the voltage at $x = 0$.

Now, these constituent subsections, i.e., multiple divisions, should be cascaded by following the procedure set forth in Section III-B. The improved accuracy gained by following this technique is numerically demonstrated in Section IV.

It should be noted that different strategies can be chosen for breaking the whole structure into its constituent multiple divisions. For instance, the overall structure can be uniformly divided into subsections of equal lengths. This approach is called the technique of geometrically uniform multiple divisions. However, this is not always the best choice, and it can be shown that, with a fixed number of constituent subsections,

$$\mathbf{T}_i = \frac{1}{2}\begin{bmatrix} \dfrac{\sqrt{Z(x_i^-)}}{\sqrt{Z(x_i^+)}} + \dfrac{\sqrt{Z(x_i^+)}}{\sqrt{Z(x_i^-)}} & \left\{\dfrac{\sqrt{Z(x_i^-)}}{\sqrt{Z(x_i^+)}} - \dfrac{\sqrt{Z(x_i^+)}}{\sqrt{Z(x_i^-)}}\right\} \exp\left(+j2\int_0^{x_i}\beta(x)dx\right) \\ \left\{\dfrac{\sqrt{Z(x_i^-)}}{\sqrt{Z(x_i^+)}} - \dfrac{\sqrt{Z(x_i^+)}}{\sqrt{Z(x_i^-)}}\right\} \exp\left(-j2\int_0^{x_i}\beta(x)dx\right) & \dfrac{\sqrt{Z(x_i^-)}}{\sqrt{Z(x_i^+)}} + \dfrac{\sqrt{Z(x_i^+)}}{\sqrt{Z(x_i^-)}} \end{bmatrix} \tag{21}$$

$$\mathbf{T}_i = \frac{1}{2}\begin{bmatrix} \left\{\dfrac{\sqrt{Z(x_i^-)}}{\sqrt{Z(x_i^+)}} + \dfrac{\sqrt{Z(x_i^+)}}{\sqrt{Z(x_i^-)}}\right\} \exp\left[-j\int_{x_{i-1}}^{x_i}\beta(x)dx\right] & \left\{\dfrac{\sqrt{Z(x_i^-)}}{\sqrt{Z(x_i^+)}} - \dfrac{\sqrt{Z(x_i^+)}}{\sqrt{Z(x_i^-)}}\right\} \exp\left[j\int_{x_{i-1}}^{x_i}\beta(x)dx\right] \\ \left\{\dfrac{\sqrt{Z(x_i^-)}}{\sqrt{Z(x_i^+)}} - \dfrac{\sqrt{Z(x_i^+)}}{\sqrt{Z(x_i^-)}}\right\} \exp\left[-j\int_{x_{i-1}}^{x_i}\beta(x)dx\right] & \left\{\dfrac{\sqrt{Z(x_i^-)}}{\sqrt{Z(x_i^+)}} + \dfrac{\sqrt{Z(x_i^+)}}{\sqrt{Z(x_i^-)}}\right\} \exp\left[j\int_{x_{i-1}}^{x_i}\beta(x)dx\right] \end{bmatrix} \tag{22}$$

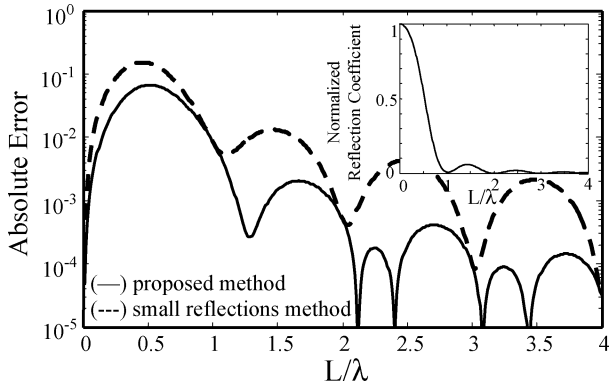

Fig. 4. Error of the normalized reflection coefficient versus normalized frequency for a triangular tapered line with $Z_0 = 50$ and $Z_L = 300$. Inset: normalized reflection coefficient versus normalized frequency.

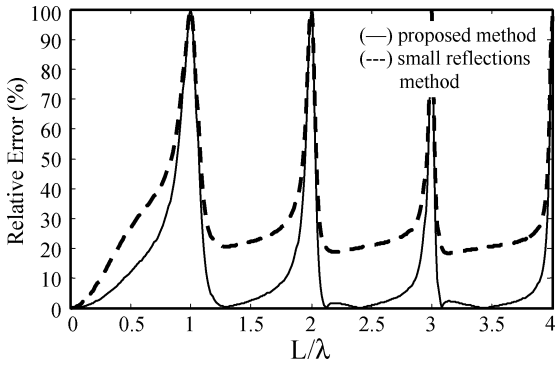

Fig. 5. Relative error of the normalized reflection coefficient versus normalized frequency for the triangular tapered line analyzed in Fig. 4.

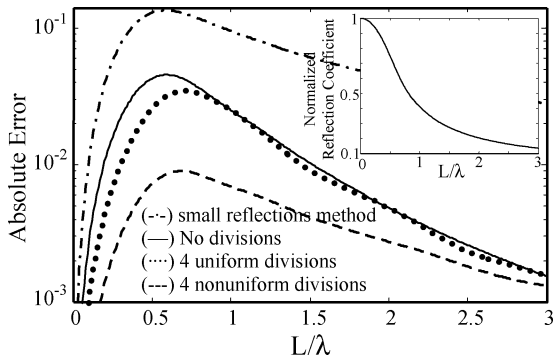

Fig. 6. Error of the normalized reflection coefficient versus normalized frequency for an exponential tapered line with $Z_0 = 50$ and $Z_L = 300$. Inset: normalized reflection coefficient versus normalized frequency.

an appropriate strategy of dividing the structure into subsections of different lengths can lead to better results. One other approach whose superiority over the geometrically uniform division strategy is shown in Section IV is the one for which the following criterion is considered in breaking the entire transmission line into its N constituent subsections:

$$\frac{Z_i^b}{Z_i^e} = \left(\frac{Z_0}{Z_L}\right)^{\frac{1}{N}}. \tag{23}$$

Here, Z_i^b and Z_i^e denote the impedance at the beginning and end of the ith subsection, respectively. It should be also noticed that

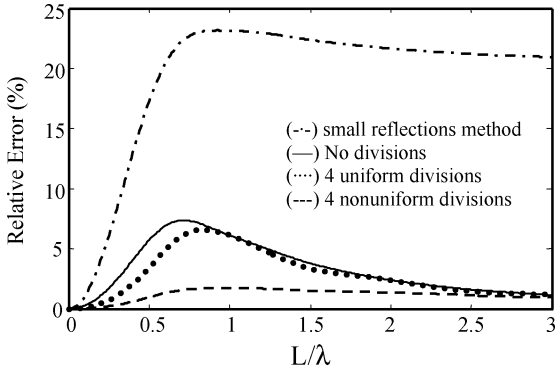

Fig. 7. Relative error of the normalized reflection coefficient versus normalized frequency for the exponential tapered line analyzed in Fig. 6.

TABLE I
TEST CIRCUIT PARAMETERS [15]

Circuit	A	B	C	D	E
Substrate	Ultralam	Ultralam	TMM	TMM	FR4
ε_r	2.6	2.6	9.8	9.8	4.1
Loss Tan	.0022	.0022	.0020	.0020	.035
Conductivity	Cu	Cu	Cu	Cu	Cu
Thickness(T)	.67	.67	1.34	1.34	1.34
Height(H)	30	30	25	25	30
W_{max}	200	200	200	200	200
W_{min}	81.7	81.7	23.6	23.6	59.6
L	1500	3000	1500	1500	1800
L_1	250	500	250	250	100
CKT Type	I	II	I	II	II

All lengths in mils.

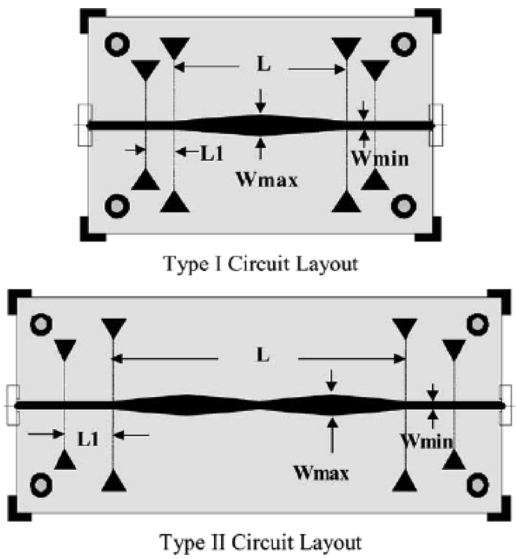

Fig. 8. Microstrip circuits used for experimental verification of the proposed method [15].

$Z_0 = \mathrm{Z}(0)$, $Z_L = \mathrm{Z}(\mathrm{L})$, and N stands for the total number of divisions. In this paper, this technique has been referred to as the technique of electrically uniform multiple divisions. Employing such an approach in breaking the whole transmission line into N subsections results in multiple divisions, whose ratios of impedance values at the beginning and at the end of it, i.e., Z_i^b/Z_i^es for different values of i, are equal to each other.

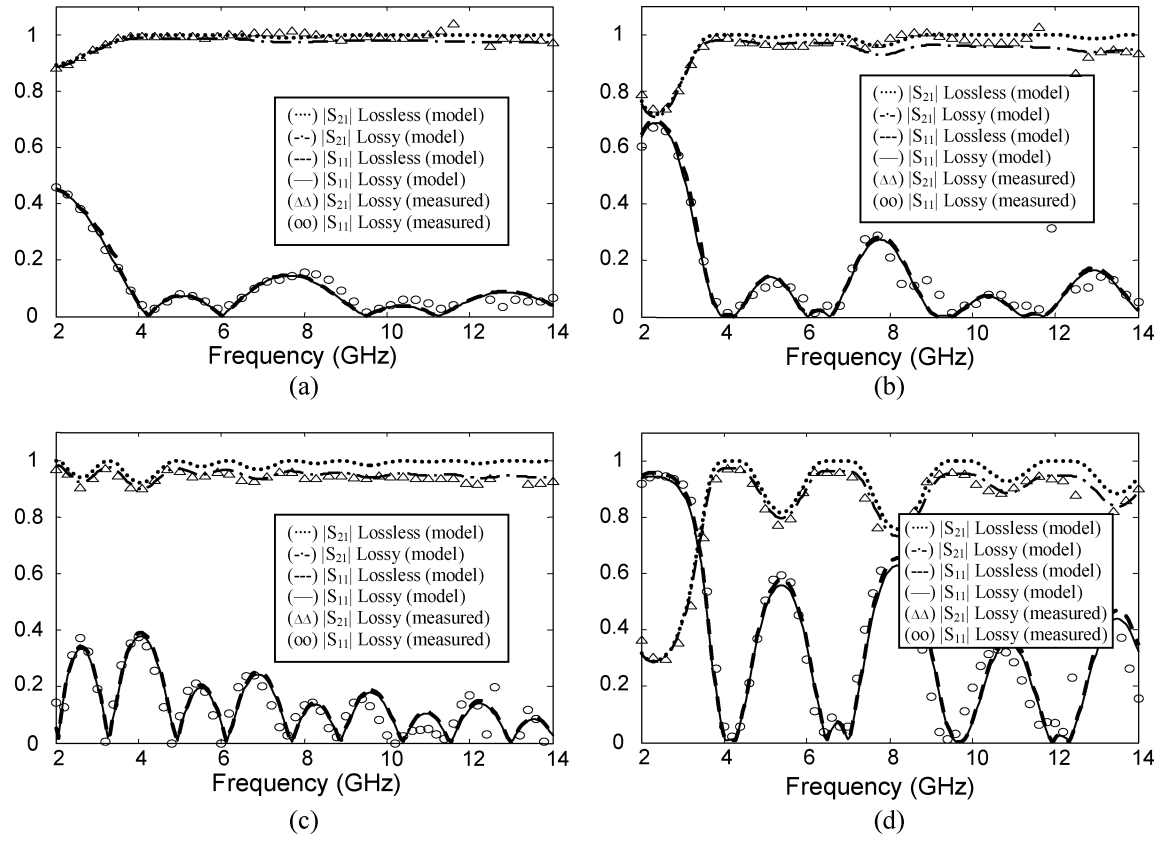

Fig. 9. Scattering parameters of test circuits A–D on low-loss substrates versus frequency: (a) circuit A, (b) circuit B, (c) circuit C, and (d) circuit D. Results of measurements are extracted from [15].

As for the accuracy of the proposed method depending on the contrast of impedance variations within the line, this way of dividing the line into several cascaded subsections heuristically seems more efficient compared with other possible approaches of multiple divisions.

IV. Nonuniform Transmission Lines

Here, the applicability of the proposed method in obtaining voltage/current distributions and tapered line characteristics are investigated by analyzing some specific examples of nonuniform transmission lines. The superiority of our analytical method to the widely used small reflections method [1] is also shown. Furthermore, the improvement obtained by following the technique of multiple divisions is numerically demonstrated. The results obtained by following the conventional numerical method of cascading uniform transmission lines [7], [8], [25] are used to examine those results obtained by applying our method.

The first example to be studied is a tapered line with the characteristic impedance given by

$$Z=\begin{cases} Z_0 e^{\left[2(x/L)^2\right]\ln(Z_L/Z_0)}, & 0\le x\le \frac{L}{2} \\ Z_0 e^{(4x/L-2x^2/L^2-1)\ln(Z_L/Z_0)}, & \frac{L}{2}\le x\le L \end{cases} \tag{24}$$

where L, Z_L, and Z_0 stand for the length of the transmission line, the load impedance, and the reference impedance, respectively. In accordance with [1], this profile is associated with a tapered line of triangular distribution, where $d(\ln(Z))/\mathrm{d}x$ is a triangular function. This profile is plotted in Fig. 2. Fig. 3(a) and (b) shows the polar locus of voltage and current along the tapered line for $L/\lambda = 1.4$, $Z_0 = 50$, and $Z_L = 100$. Here, the voltage is normalized to the value of voltage at $x = 0$. In Fig. 4, the incurred error of calculating a normalized reflection coefficient by following our approach and the method of small reflections is plotted versus normalized frequency. Also, the relative error, in percentages, is shown in Fig. 5. These figures clearly demonstrate the superiority of our method over the method of small reflections. This example can also be analyzed by the method introduced in [24]. The result is not considerably different from the results of the proposed method. The maximum relative difference between the results of two methods is at most as high as $10^{-3}\%$.

As another example, a tapered line with the following characteristic impedance is considered:

$$Z = Z_0 e^{(x/L)^4 \ln(Z_L/Z_0)}. \tag{25}$$

Again, L, Z_L, and Z_0 denote the length of the transmission line, the load impedance, and the reference impedance, respectively. Also, it is assumed that $Z_0 = 50$ and $Z_L = 300$. This profile is associated with the tapered line of exponential distribution [1] and is shown in Fig. 2. In Fig. 6, the incurred error of computing the normalized reflection coefficient versus normalized frequency is plotted, where four different methods, i.e., the small reflections method, the differential transfer matrix with no divisions, the technique of cascading four geometrically uniform divisions (four uniform divisions), and the technique

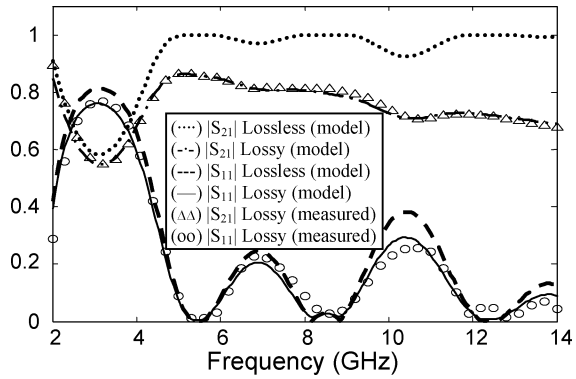

Fig. 10. Scattering parameters of test circuit E on lossy substrate versus frequency; results of measurement are extracted from [15].

of cascading four electrically uniform divisions (four nonuniform divisions), are compared with each other. Also, the corresponding relative error, in percentages, is plotted in Fig. 7. These figures noticeably demonstrate the superiority of using the criterion (23) in applying the technique of multiple divisions.

V. Tapered Microstrip Lines

Tapered microstrip lines have been extensively used in many applications and play an important role in microwave engineering. These lines can be characterized by simple circuit models, whenever the fringing fields are negligible and only the dominant or quasi-TEM modes propagate along the line. In this section, the model derived by Hammerstad and Jensen [26] is employed to obtain the variation of the microstrip effective dielectric constant and characteristic impedance as a function of the width-to-height ratio W/H, and then different microstrip circuits are analyzed. It should be noted that this model also takes the nonzero strip thickness and dispersion into account.

Five circuits, which were recently analyzed by Edwards *et al.* [15], are considered to verify the accuracy of our proposed method. These circuits, adapting the nomination of [15], are designated as circuits A-E. Table I recapitulates the parameters of these circuits. Two circuit configurations used in these experiments are shown in Fig. 8. Figs. 9(a)–(d) and 10 show the obtained results of test circuits A-D on low-loss substrates and those of test circuit E on moderately lossy substrate, respectively. Results of the measurements are those given in [15]. Our results are in excellent agreement with experimental results. In particular, compared with the results given in [15], following our approach seems to render simulation results of better accuracy, especially for test circuits C and D. This point can be explained by considering the fact that none of the simplifying assumptions made in [15], i.e., linearly varying effective permittivity ε_{eff} and linearly varying logarithm of characteristic impedance $\ln(Z)$, are employed in our proposed method.

VI. Conclusion

A new analytical method has been introduced for analyzing tapered transmission lines. This method is based on a suitable expansion of voltage distribution with unknown coefficients obtained by following a method similar to conventional and modified differential transfer matrix methods already employed for the analysis of optical structures, where no simplifying assumption is made and a rigorous approach is followed. Reflection and transmission coefficients were derived, the method of analyzing cascaded structures was presented, and the techniques of multiple divisions for improving the accuracy of the proposed method were also introduced. The applicability of the proposed method and its superiority to the well-known small reflections method was shown via several numerical examples. In particular, nonuniform lossy/lossless microstrip lines were investigated by following our proposed method.

References

[1] R. E. Collin, *Foundations for Microwave Engineering*. New York: McGraw-Hill, 1992.
[2] S. C. Burkhart and R. B. Wilcox, "Arbitrary pulse shape synthesis via nonuniform transmission lines," *IEEE Trans. Microw. Theory Tech.*, vol. 38, no. 10, pp. 1514–1518, Oct. 1990.
[3] N. H. Younan, B. L. Cox, C. D. Taylor, and W. D. Rather, "An exponentially tapered transmission line antenna," *IEEE Trans. Electromagn. Compat.*, vol. 36, no. 1, pp. 141–144, Feb. 1994.
[4] C. E. Baum and J. M. Lehr, "Tapered transmission-line transformers for fast high-voltage transients," *IEEE Trans. Plasma Sci.*, vol. 30, no. 5, pt. 1, pp. 1712–1721, Oct. 2002.
[5] D. K. Misra, *Radio-Frequency and Microwave Communication Circuits: Analysis and Design*. New York: Wiley, 2001.
[6] L. A. Hayden and V. K. Tripathi, "Nonuniformly coupled microstrip filters for analog signal processing," *IEEE Trans. Microw. Theory Tech.*, vol. 39, no. 1, pp. 47–53, Jan. 1991.
[7] J. E. Schutt-Aine, "Transient analysis of nonuiform transmission lines," *IEEE Trans. Circuits Syst.*, vol. 39, no. 5, pp. 378–385, May 1992.
[8] T. Dhaene, L. Martens, and D. D. Zutter, "Transient simulation of arbitrary nonuniform interconnection structures characterized by scattering parameters," *IEEE Trans. Circuits Syst.*, vol. 39, no. 11, pp. 928–937, Nov. 1992.
[9] V. Dvorak, "Computer simulation of signal propagation through a nonuniform transmission line," *IEEE Trans. Microw. Theory Tech.*, vol. MTT-33, no. 9, pp. 1210–1212, Sep. 1973.
[10] T. Kashiwa, M. Sasaki, S. Maeda, and I. Fukai, "Full wave analysis of tapered microstrip lines using the conformal grids FD-TD method," in *IEEE MTT-S Int. Microw. Symp. Dig.*, 1992, pp. 1213–1216.
[11] C. W. Hsue and C. D. Hechtman, "Transient analysis of non-uniform high pass transmission lines," *IEEE Trans. Microw. Theory Tech.*, vol. 38, no. 8, pp. 1023–1030, Aug. 1990.
[12] C. W. Hsue, "Time-domain scattering parameters of an exponential transmission lines," *IEEE Trans. Microw. Theory Tech.*, vol. 39, no. 11, pp. 1891–1895, Nov. 1991.
[13] P. Bouchard and R. J. Gagne, "Transient analysis of lossy parabolic transmission lines with nonlinear loads," *IEEE Trans. Microw. Theory Tech.*, vol. 43, no. 6, pp. 1330–1333, Jun. 1995.
[14] M. J. Ahmed, "Impedance transformation for exponential, cosine-squared, and parabolic tapered transmission lines," *IEEE Trans. Microw. Theory Tech.*, vol. MTT-29, no. 6, pp. 67–68, Jun. 1981.
[15] C. L. Edwards, M. L. Edwards, S. Cheng, R. K. Stilwell, and C. C. Davis, "A simplified analytic CAD model for linearly tapered microstrip lines including losses," *IEEE Trans. Microw. Theory Tech.*, vol. 52, no. 3, pp. 823–830, Mar. 2004.
[16] H. Curtins and A. V. Shah, "Step response of lossless nonuniform transmission lines with power law characteristic impedance function," *IEEE Trans. Microw. Theory Tech.*, vol. MTT-33, no. 11, pp. 1210–1212, Nov. 1985.
[17] J. P. Mahon and R. S. Elliott, "Tapered transmission lines with a controlled ripple response," *IEEE Trans. Microw. Theory Tech.*, vol. 21, no. 9, pp. 580–583, Sep. 1990.
[18] Y. Wang, "New method for tapered transmission line design," *Electron. Lett.*, vol. 27, pp. 2396–2398, 1991.
[19] R. E. Collin, "The optimum tapered transmission line matching section," *Proc. IRE*, vol. 44, no. 4, pp. 539–548, Apr. 1956.
[20] S. Khorasani and K. Mehrany, "Differential transfer-matrix method for solution of one-dimensional linear nonhomogeneous optical structures," *J. Opt. Soc. Amer. B, Opt. Phys.*, vol. 20, pp. 91–96, 2003.
[21] S. Khorasani and A. Adibi, "New analytical approach for computation of band structure in one-dimensional periodic media," *Opt. Commun.*, vol. 216, pp. 439–451, 2003.

[22] M. H. Eghlidi, K. Mehrany, and B. Rashidian, "Modified differential transfer matrix method for solution of one dimensional linear inhomogeneous optical structures," *J. Opt. Soc. Amer. B, Opt. Phys.*, vol. 22, pp. 1521–1528, 2005.
[23] K. Mehrany and S. Khorasani, "Analytical solution of non-homogeneous anisotropic wave equations based on differential transfer matrix method," *J. Opt. A., Pure Appl. Opt.*, vol. 4, pp. 624–635, 2002.
[24] B. Faraji, M. H. Eghlidi, K. Mehrany, and B. Rashidian, "Analytical approach for analyzing tapered transmission lines," in *Proc. Eur. Circuit Theory Des. Conf.*, 2005, vol. 3, pp. III/181–III/184.
[25] K. N. S. Rao, V. Mahadevan, and S. P. Kosta, "Analysis of straight tapered mirostrip lines—ASTMIC," *IEEE Trans. Microw. Theory Tech.*, vol. MTT-25, no. 2, p. 164, Feb. 1977.
[26] E. Hammerstad and O. Jensen, "Accurate model for microstrip computer aided design," in *IEEE MTT-S Int. Microw. Symp. Dig.*, 1980, pp. 407–409.

Mohammad Hadi Eghlidi was born in Shiraz, Iran, in 1980. He received the B.Sc. and M.Sc. degrees in electrical engineering from Sharif University of Technology, Tehran, Iran, in 2002 and 2005, respectively.

He is currently with the Technical Faculty of Christian-Albrechts-Universität, Kiel, Germany. His research interests include analytical and numerical methods in electromagnetic and optics and analysis and applications of composite magnetic materials.

Khashayar Mehrany was born in Tehran, Iran, on September 16, 1977. He received the B.Sc., M.Sc., and Ph.D. (*magna cum laude*) degrees from Sharif University of Technology, Tehran, Iran, in 1999, 2001, and 2005, respectively, all in electrical engineering.

Since then, he has been an Assistant Professor with the Department of Electrical Engineering, Sharif University of Technology. His research interests include photonics, semiconductor physics, nanoelectronics, and numerical treatment of electromagnetic problems.

Bizhan Rashidian received the B.Sc. and M.Sc. (with the highest honor) degrees from Tehran University, Tehran, Iran, in 1987 and 1989, respectively, and the Ph.D. degree from the Georgia Institute of Technology, Atlanta, in 1993, all in electrical engineering.

Since 1994, he has been with the Department of Electrical Engineering, Sharif University of Technology, Tehran, Iran, where he is currently a Professor. He is also the Founding Director of the Microtechnology Laboratory, Nanoelectronics Laboratory, and the Photonics Laboratory. His active research areas include optics, nanoelectronics, micromachining, microelectronics, and ultrasonic.